20 August 1998

PHYSICS LETTERS B

ELSEVIER

Physics Letters B 434 (1998) 14–20

Comparative quadrupole moments of superdeformed bands in $^{193-196}$Pb

U.J. van Severen [a], R.M. Clark [b], R. Krücken [b,1], H. Hübel [a], S.J. Asztalos [b], J.A. Becker [d], B.C. Busse [b], M.A. Deleplanque [b], R.M. Diamond [b], P. Fallon [b], K. Hauschild [d], I.M. Hibbert [c], I.Y. Lee [b], A.O. Macchiavelli [b], R.W. MacLeod [b], G. Schmid [b], F.S. Stephens [b], K. Vetter [b], R. Wadsworth [c], S. Wan [e]

[a] *Institut für Strahlen- und Kernphysik, Universität Bonn, D 53115 Bonn, Germany*
[b] *Lawrence Berkeley National Laboratory, Berkeley, CA 94720, USA*
[c] *Department of Physics, University of York, Heslington, York YO15DD, UK*
[d] *Lawrence Livermore National Laboratory, Livermore, CA 94550, USA*
[e] *Gesellschaft für Schwerionenforschung mbH, 64291 Darmstadt, Germany*

Received 19 March 1998; revised 20 May 1998
Editor: R.H. Siemssen

Abstract

Lifetimes have been measured for states in five superdeformed yrast bands in $^{193-196}$Pb using the Gammasphere spectrometer array. Centroid shifts and lineshapes of transitions showing attenuated Doppler shifts have been analyzed. Transition quadrupole moments are deduced for the five bands including, for the first time, bands of two odd-A Pb isotopes. The quadrupole moments are found to be remarkably similar for the yrast bands in ^{194}Pb (band 1), ^{195}Pb (bands 1 and 2) and ^{196}Pb (band 1) ($Q_t \approx 20$ b). However, for ^{193}Pb a smaller value, $Q_t = 17.3(7)$ b, is obtained. This can be explained in terms of the occupation of the neutron N = 7 intruder orbitals. © 1998 Elsevier Science B.V. All rights reserved.

PACS: 21.10.Re; 23.20.Ck; 27.80.+w

A large number of superdeformed (SD) rotational bands have been discovered in recent years in the mass 190 region [1]. However, most of them are not connected to lower-lying states of known excitation energy, spin and parity. Therefore, their nucleon-configuration assignments are generally based only on the systematic behaviour of properties like the dynamic moments of inertia and the transition quadrupole moments. While the influence of the intruder orbitals on the moments of inertia is well documented, their impact on the quadrupole moments could only be probed recently as high-precision data obtained with large γ-ray spectrometer arrays became available [2–7] and comparative measurements under identical experimental conditions could be performed.

The Hg–Pb region is known for SD bands which show an increase of the dynamic moments of inertia

[1] Present address: W.A. Wright Nuclear Structure Laboratory, Yale University, New Haven, CT 06520, USA.

PII: S0370-2693(98)00819-3

$\Im^{(2)}$ with rotational frequency. Bands with rather constant $\Im^{(2)}$ also exist. Such differences in the behaviour of the dynamic moments of inertia have been used to assign the high-N intruder configurations to the bands. This region is also known for a large number of identical SD bands. Long sequences of γ-ray transitions with either the same energies or with energies obeying a fixed relation with respect to the energies of a SD band in a neighbouring nucleus exist. This observation led to the suggestion of quantized alignments between different bands [8].

Quadrupole moments deduced from measured lifetimes have been reported [2–4,9–14] for several SD bands in the Hg–Pb region. They remain remarkably constant as a function of rotational frequency [see e.g. Ref. 4] within a given band. This proves that the deformation remains stable despite the increasing moments of inertia with increasing frequency. Consequently the increase in $\Im^{(2)}$ was attributed to a gradual alignment of $j_{15/2}$ neutrons followed by the alignment of $i_{13/2}$ protons, accompanied by a pairing decrease [15,16]. However, the lifetime data for different isotopes were generally obtained in experiments using different Doppler-shift techniques and under different experimental conditions. It is therefore difficult to compare the results for SD bands in different nuclei. The high efficiency of the new large γ-ray spectrometer arrays makes it possible, for the first time, to perform lifetime measurements with high accuracy. It is possible to obtain data on SD bands simultaneously for neighbouring nuclei produced in the same experiment under nearly identical conditions. The deduced relative quadrupole moments are then freer of systematic uncertainties like insufficient knowledge of the stopping powers and different treatment of the side feeding.

We have measured the lifetimes of states in five SD bands in $^{193-196}$Pb using Doppler-shift attenuation methods. From centroid shifts and from lineshapes of the SD transitions quadrupole moments are deduced. Our work represents the first comparative determination of transition quadrupole moments for SD bands in odd- and even-mass Pb nuclei.

High-spin states in neutron-deficient Pb isotopes were populated in the ^{172}Yb(^{26}Mg,xn)^{192,193}Pb, ^{174}Yb(^{26}Mg,xn)^{194,195}Pb and ^{176}Yb(^{26}Mg,xn)^{196,197}Pb reactions at beam energies of 139, 137 and 135 MeV, respectively. The ^{26}Mg beams were accelerated by the LBNL 88-Inch Cyclotron. The targets consisted of approximately 1 mg/cm^2 of enriched Yb isotopes on 12 mg/cm^2 Pb backings. Gamma-ray coincidences were measured with the Gammasphere array [17]. For this experiment it consisted of 98 large-volume Compton-suppressed Ge detectors situated at the following angles relative to the beam direction: 17.3°, 31.7°, 37.4°, 50.1°, 58.3°, 69.8°, 79.2°, 80.7°, 90.0°, 99.3°, 100.8°, 110.2°, 121.7°, 129.9°, 142.6°, 148.3°, 162.7°. In a measuring time of about 24 h for each reaction totals of about $9 \cdot 10^8$ four- and higher-fold events were collected on magnetic tape. In the off-line analysis coincidence spectra for the forward and backward detectors were produced by setting three energy gates on uncontaminated lines in any of the other detectors. In this way spectra were incremented for all known SD bands in the six isotopes from ^{192}Pb to ^{197}Pb. However, only the yrast bands in $^{193-196}$Pb showed sufficient statistics for a reliable lifetime analysis. As an example, a pair of spectra from the forward and backward detectors is shown in Fig. 1 for the yrast SD band in ^{196}Pb. Spectra for the 90° and near-90° detectors were also produced and used to locate contaminations at the positions of the shifted peaks in the spectra from the forward or backward detectors.

Two Doppler-Shift Attenuation Methods (DSAM) were applied in the analysis of the data: centroid shifts and lineshapes were used to deduce lifetimes in five of the SD bands. First, we want to describe the centroid-shift method. From the centroids of the γ-ray lines in the spectra fractional Doppler-shifts, $F(\tau)$, were obtained, where $F(\tau)$ is the ratio $v(\tau)/v_0$ of the average recoil velocity, at which a state decays, to the initial recoil velocity and τ is the lifetime of a given state. The initial recoil velocities were $v_0/c = 1.41\%$, 1.38% and 1.36% for ^{193}Pb, ^{194,195}Pb and ^{196}Pb, respectively. The experimental $F(\tau)$ curves extracted for each of the SD bands which were sufficiently populated in our experiment are displayed in Fig. 2. Calculated $F(\tau)$ curves, assuming a rotational cascade with a constant quadrupole moment, are shown for comparison with the data. The electronic stopping powers were calculated using the tables of Ziegler et al. [18] and the nuclear component to the stopping was treated according to the theory of Lindhard et al. [19]. Table 1

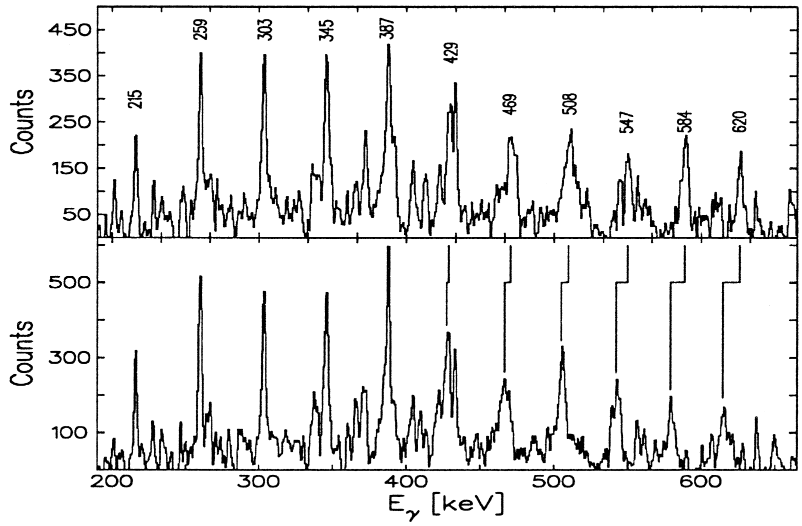

Fig. 1. Triple gated spectra for the SD yrast band in ^{196}Pb obtained at forward angles (upper spectrum) and backward angles (lower spectrum). Energies are given in keV.

summarizes the quadrupole moments for each of the bands extracted through a χ^2-minimization fit of the calculated curves to the data. The transition quadrupole moments Q_t were derived under the assumption that the side feeding quadrupole moments Q_{sf} have the same values as Q_t. This usually re-

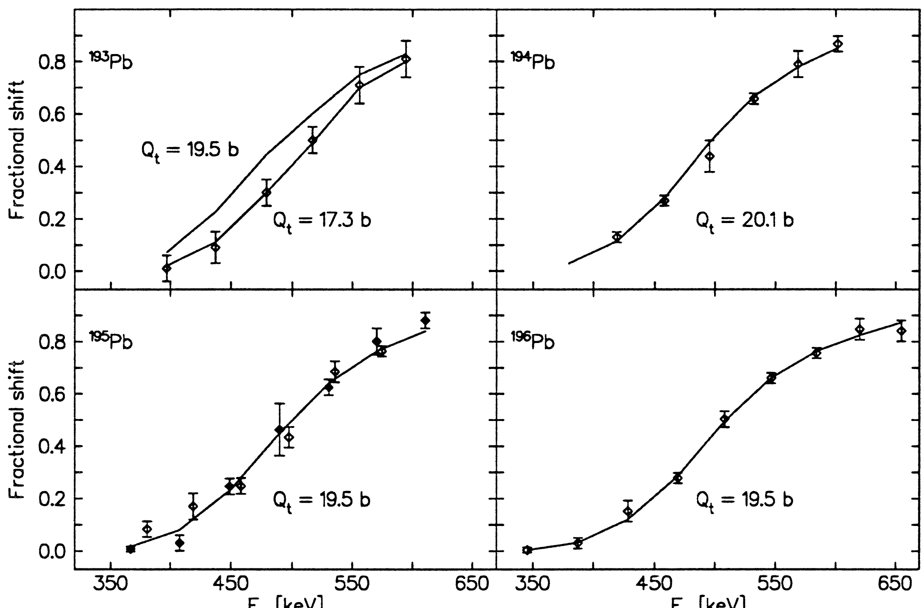

Fig. 2. Fractional Doppler shifts F(τ) for the SD yrast bands in $^{193-196}$Pb. The open and full symbols in the lower left panel are for bands 1 and 2 in ^{195}Pb, respectively. The second curve in the upper left panel calculated with $Q_t = 19.5\,b$ is shown to demonstrate the smaller experimental Q_t value for ^{193}Pb.

Table 1
Transition quadrupole moments Q_t, extracted in the present work and in previous studies

Nucleus	Band	Q_t [b] centroid shift	Q_t [b] line shape	Q_t [b] prev. work
^{193}Pb	SD1	$17.3^{+0.7}_{-0.6}$	–	–
^{194}Pb	SD1	$20.1^{+0.3}_{-0.5}$	20.7 ± 1.9	20.2 ± 1.3 $^{(a)}$
^{195}Pb	SD1	$19.5^{+1.0}_{-0.9}$	20.7 ± 2.2	–
^{195}Pb	SD2	$19.5^{+0.9}_{-1.0}$	20.2 ± 2.1	–
^{196}Pb	SD1	$19.5^{+0.4}_{-0.3}$	20.9 ± 2.0	18.3 ± 3.0 $^{(b)}$

$^{(a)}$ Ref. [9,10] $^{(b)}$ Ref. [11]

sulted in the lowest χ^2 value, except for ^{193}Pb where the absolute χ^2 minimum is obtained for $Q_t/Q_{sf} = 15.9/23.3$. However, we adopt $Q_t = 17.3(7)$ b, which is derived with the restriction $Q_t = Q_{sf}$, resulting in a somewhat larger χ^2. A side feeding cascade of five transitions was used with constant $\Im^{(2)}$ moments of inertia of $\Im^{(2)}_{sf} = 110$ $\hbar^2$/MeV for ^{194,196}Pb and $\Im^{(2)}_{sf} = 100$ $\hbar^2$/MeV for ^{193,195}Pb, corresponding to the moments of inertia of the SD bands around a rotational frequency of $\hbar\omega = 0.25$ MeV. A variation of $\Im^{(2)}$ had little effect on the quadrupole moments. The errors of the Q_t values given in Table 1 include these systematic uncertainties, but they do not include those introduced by the stopping powers. Thus, the uncertainties represent the accuracy to which the different values can be compared to each other.

For the yrast bands in ^{194}Pb and ^{196}Pb and for bands 1 and 2 in ^{195}Pb DSAM lineshapes could be analysed. A program based on the one developed by Bacelar et al. [20] and modified by Gascon et al. [21] was used. The analysis is carried out in three steps. In a first step, a Monte Carlo simulation of 6000 histories of nuclei recoiling through the Yb target and Pb stopper foils is performed. This results in statistical velocity distributions at about 600 different times, which corresponds to time intervals of 2 fs. In the second step, the detector geometry is taken into account and, using the velocity distributions calculated in the first step and the stopping powers [18,19], a line shape for each decay time is obtained. In the final step, the theoretical line shapes are fitted to the experimental ones in a χ^2-minimization with the quadrupole moments as free parameters. The side feeding was again modelled by rotational cascades of five transitions with energies calculated using the moments of inertia given above.

As an example, the measured lineshapes for two transitions of the yrast SD band in ^{196}Pb and the results of the fits are shown in Fig. 3. Two different fitting procedures were carried out: (i) the lineshapes of each transition was fitted individually, starting from the top of the bands and using the lifetime and feeding time of each state as input for the subsequent level; (ii) the lineshapes of all transitions were fitted simultaneously, starting with the top level and adding

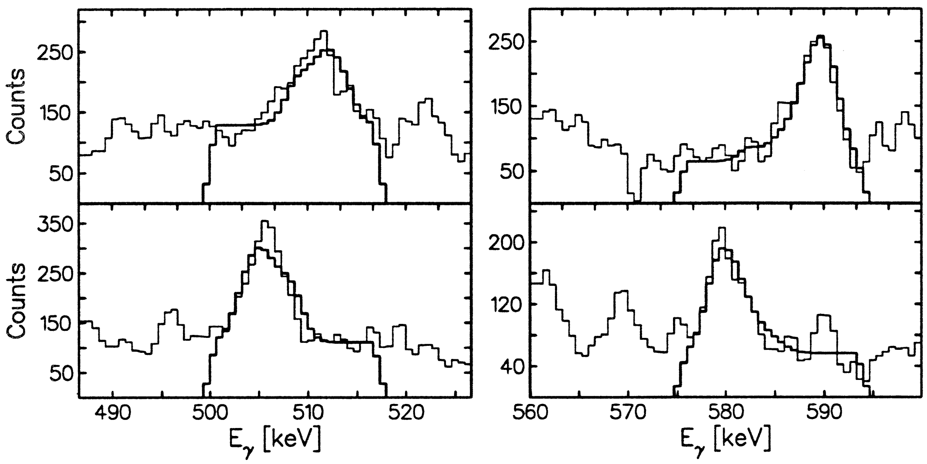

Fig. 3. Sample lineshapes of the 508 and 584 keV SD transitions of the SD yrast band in ^{196}Pb. Transitions shown in the top panel correspond to forward angles, the lower panel shows the same transitions for backward angles. The fitted lineshapes are drawn as thick curves.

the lower lying states until all states were included. The results for both approaches are in agreement. In the fits, the transition quadrupole moments Q_t and the side-feeding quadrupole moments Q_{sf} were used as free parameters. The resulting Q_{sf} values turned out to be equal to Q_t or about 10% smaller than Q_t. The Q_t values obtained in this way are also included in Table 1. They are averages for the different transitions that could be analyzed for each band.

The most striking observation, when comparing the quadrupole moments given in Table 1, is their remarkable similarity for ^{194,195,196}Pb and the sudden drop for ^{193}Pb. We have to conclude that the SD potential-energy minimum is very stable and the deformation does not change, within our experimental accuracy, for the heavier isotopes. However, for ^{193}Pb the deformation seems to be significantly lower. This observation is independent of the fact whether moments of inertia are equal or different (or whether transition energies are identical or not).

The difference in deformation between ^{193}Pb and the heavier Pb isotopes may be explained as a result of the different occupation of N = 7 neutron intruder orbitals. The configurations of the SD bands are most easily discussed looking at the neutron single-particle routhians presented in Fig. 4. One has to note, however, that pair correlations play an important role at superdeformation in this mass region. The relevant quasi-particle diagrams may be found in the literature. The basic conclusions do not change when working in a single-particle or in a quasi-particle picture. As the Fermi level moves up with increasing neutron number, we have to assume that an increasing number of N = 7 orbitals will be occupied. Within the single-particle picture the high-N neutron intruder configurations of the yrast SD bands summarized in Table 2 are expected. They explain the behaviour of the dynamic moments of inertia, the routhians with their signature splitting and the spins (as obtained by the spin-fitting method). For the yrast signature-partner bands in the odd-A isotopes ^{193}Pb and ^{195}Pb the dynamic moments of inertia $\Im^{(2)}$ do not show the rise with increasing frequency that is otherwise characteristic for the SD bands in this mass region. This suggests the occupation of a single N = 7 orbital by the odd neutron which reduces pair correlations and blocks the alignment of a pair of neutrons in that orbital. For ^{193}Pb that would be the 7_2 and for ^{195}Pb the 7_3 orbital which lie close to the Fermi level in the two nuclei. This agrees with the observed signature splitting which is much larger for the N = 7_2 orbital in ^{193}Pb

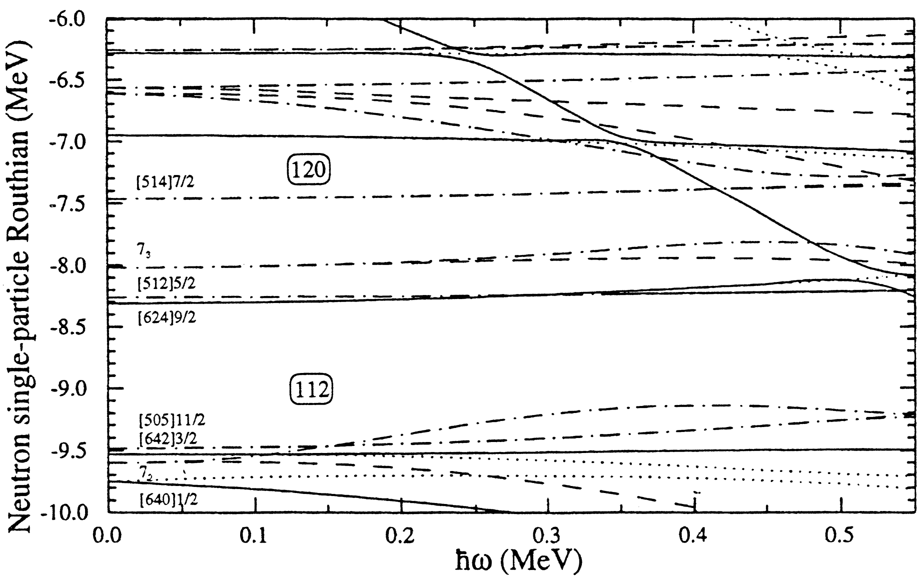

Fig. 4. Neutron single-particle routhians calculated for a deformed Woods–Saxon potential with $\beta_2 = 0.495$, $\beta_4 = 0.060$, $\gamma = 0°$, The orbitals are labeled by their asymptotic Nilsson quantum numbers $[Nn_3\Lambda]\Omega$ or, in the case of high-N intruder orbitals, by N_i.

Table 2
N = 7 neutron intruder-orbital configuration of the lowest-energy SD bands in $^{193-196}$Pb

^{193}Pb	^{194}Pb	^{195}Pb	^{196}Pb
$\nu 7_1(2)7_2(1)$	$\nu 7_1(2)7_2(2)$	$\nu 7_1(2)7_2(2)7_3(1)$	$\nu 7_1(2)7_2(2)$

compared to that of the N = 7_3 orbital in ^{195}Pb. For the even-A isotopes ^{194}Pb and ^{196}Pb $\mathfrak{J}^{(2)}$ is increasing with about the same slope indicating the same occupation of N = 7 intruder orbitals. The difference between these two nuclei is then the occupation of the [512]5/2 or [624]9/2 orbitals by a neutron pair in ^{196}Pb. These orbitals show no alignment in the observed frequency range, see Fig. 4, and therefore do not influence the $\mathfrak{J}^{(2)}$ moment of inertia.

The quadrupole moments observed in our work are in agreement with this interpretation. The intruder orbitals N = 7_1 (of [770]1/2 origin) and 7_2 (of [761]3/2 origin) are strongly down-sloping as a function of deformation and, thus, are strongly prolate deformation driving. The higher-lying N = 7_3 (of [752]5/2 origin) as well as the [512]5/2 and [624]9/2 orbitals show much less deformation-driving effects. The smaller deformation that we observe for ^{193}Pb compared to the heavier isotopes is then due to the difference in the occupation of the 7_2 orbital. In ^{193}Pb this strongly prolate driving orbital is occupied only by one neutron, whereas in ^{194,195,196}Pb there are two neutrons in this orbital.

It would be interesting to make a similar comparison of the quadrupole moments of the SD bands in the neighbouring Hg isotopes. However, the data that are available for the Hg chain of isotopes are obtained in different experiments and cannot be compared with similar confidence. In a recent experiment by Busse et al. [3] quadrupole moments have been determined for six bands in ^{193}Hg, which represents a set of comparative results in a single nucleus. The Q_t values are found to be very similar ($Q_t \approx 17$ b) for all six bands, suggesting that the active single-particle orbitals exhibit only small shape-driving effects. They are the two signatures of the [512]5/2, [624]9/2 and 7_3 orbitals that are also responsible for the yrast SD bands of the heavier Pb isotopes with the constant quadrupole moments found in our measurement. From the same experiment Busse et al. [3] deduce a quadrupole moment for the yrast SD band in ^{192}Hg of 20.2(1.2) b. This value is significantly larger than the results of previous experiments [2,4] which lie around 18 b. The reason for the discrepancy is not clear. For ^{192}Hg and ^{194}Hg, where the most accurate values exist [2], the quadrupole moments of the yrast SD bands are equal within their experimental uncertainties ($Q_t \approx$ 17.7 b). These nuclei are the isotones to ^{194}Pb and ^{196}Pb and, according to the arguments made above about their intruder-orbital configuration, are expected to show similar deformation. For ^{191}Hg ($Q_t =$ 18(3) b, [22]), which is the isotone to ^{193}Pb, the experimental uncertainty is of the same order as the effect found in our work for the Pb isotopes and which we attribute to the difference in the N = 7_2 neutron intruder configuration. For the even lighter isotope ^{190}Hg ($Q_t =$ 17.7(1.2) b, [23]) the quadrupole moment seems to be similar to the one found in the heavier Hg isotopes by most authors [2–4,14]. At present it is not clear if this reflects systematic uncertainties of the different experiments or is a real physical effect. In this mass region the situation may be complicated because pairing plays a role and this may affect details of the deformation. In the A = 150 region rather accurate data on quadrupole moments exist [6,7,24]. Here, definite changes in Q_t are observed for different high-N intruder configurations and may be accounted for by the ’’additivity principle’’ [25].

Quadrupole moments for the Pb isotopes have recently been calculated [26] using the cranked Hartree–Fock–Bogoliubov method with the Lipkin–Nogami prescription. The calculated Q_t values of 20.0, 19.8 and 19.7 b for the yrast SD bands in ^{194}Pb, ^{195}Pb and ^{196}Pb, respectively, are in excellent agreement with our measured values (see Table 1). The theory also predicts a decrease in Q_t for the yrast SD band in ^{193}Pb to 19.2 b. However, the calculated value is larger than the experimental result of 17.3(7) b.

Finally, we want to point out the different quadrupole moments for the pairs of isotones ^{192}Hg, ^{194}Pb and ^{194}Hg, ^{196}Pb, but always keeping in mind that the data have been obtained in different experiments and that discrepancies exist between the results in some cases. For ^{192}Hg Q_t values between 17.7(1.0) and 20.2(1.2) b have been measured [2–4] and for ^{194}Hg 17.7(4) b is reported [2], whereas for

^{194,196}Pb we obtain $Q_t \approx 20$ b. A difference is also found in the calculations [26] mentioned above: $Q(^{192,194}Hg) = 18.6$ b and $Q(^{194,196}Pb) \approx 19.9$ b. It may be more interesting to note that the yrast bands in ^{192}Hg and ^{194}Pb as well as those in ^{194}Hg and ^{196}Pb are identical [1] despite the difference in their quadrupole moments of about 10%. A similar observation has been made in other mass regions [5,7]. This shows that it is not necessarily an identical deformation which is responsible for the occurrence of identical bands.

In conclusion, the present work gives one of the first sets of comparative transition quadrupole moments of SD bands in neighbouring isotopes. For the first time Q_t values are obtained for odd-A Pb isotopes. The results show a remarkable stability of the SD potential energy minimum for states with the same number of $N = 7_1$ and 7_2 neutron intruder orbitals occupied in $^{194-196}$Pb and a clear difference for ^{193}Pb with one $N = 7_2$ neutron less than for the heavier neighbours.

This work was supported by the U.S. Department of Energy under Contract No. DE-AC03-76SF00098. The work of the Bonn group was supported by BMBF Germany and by NATO, that of the Yale group by UK EPSRC.

References

[1] X.L. Han, C.L. Wu,'Nuclear Superdeformation Data Tables', Nuclear Data Tables 63 (1996) 117.
[2] E.F. Moore et al., Phys. Rev. C 55 (1997) R2150.
[3] B. Busse et al., Phys. Rev. C 57 (1998) R1017.
[4] P. Willsau et al., Nucl. Phys. A 574 (1994) 560.
[5] R.M. Clark et al., Phys. Rev. Lett. 76 (1996) 3510.
[6] H. Savajols et al., Phys. Rev. Lett. 76 (1996) 4480.
[7] D. Nisius et al., Phys. Lett. B 392 (1997) 18.
[8] F.S. Stephens et al., Phys. Rev. Lett. 65 (1990) 301.
[9] P. Willsau et al., Z. Phys. A 344 (1993) 351.
[10] R. Krücken et al., Phys. Rev. C 55 (1997) R1625, and references therein.
[11] E.F. Moore et al., Phys. Rev. C 48 (1993) 2261.
[12] I.Y. Lee, Phys. Rev. C 50 (1994) 2602.
[13] J.R. Hughes et al., Phys. Rev. Lett. 72 (1994) 824.
[14] R. Kühn et al., Phys. Rev. C 55 (1997) R1002.
[15] M.A. Riley et al., Nucl. Phys. A 512 (1990) 178.
[16] M.W. Drigert et al., Nucl. Phys. A 530 (1991) 452.
[17] I.Y. Lee, Nucl. Phys. A 520 (1990) 641c.
[18] J.F. Ziegler et al., The Stopping and Ranges of Ions in Matter, Pergamon Press, London, 1985.
[19] J. Lindhard et al., K. Dan. Vidensk. Selsk. Mat. Fys. Medd. 33 (1963) 14.
[20] J.C. Bacelar et al., Phys. Rev. C 35 (1987) 1170.
[21] J. Gascon et al., Nucl. Phys. A 513 (1990) 344.
[22] M.P. Carpenter et al., Phys. Lett. B 240 (1991) 44.
[23] H. Amro et al., Phys. Lett. B 413 (1997) 15.
[24] C.W. Beausang et al., Phys. Lett. B 417 (1998) 13.
[25] W. Satula et al., Phys. Rev. Lett. 77 (1996) 5182.
[26] P.-H. Heenen, private communication.